NeuroImage: Clinical 24 (2019) 102027

Contents lists available at ScienceDirect

NeuroImage: Clinical

journal homepage: www.elsevier.com/locate/ynicl

Modular organization of brain resting state networks in patients with classical trigeminal neuralgia

Yuan-Hsiung Tsai[a], Xia Liang[b], Jen-Tsung Yang[c,d], Li-Ming Hsu[e,*]

[a] Department of Diagnostic Radiology, Chang Gung Memorial Hospital at Chiayi, Chiayi, Taiwan
[b] Laboratory for Space Environment and Physical Sciences, Harbin Institute of Technology, Harbin 150001, China
[c] Department of Neurosurgery, Chang Gung Memorial Hospital at Chiayi, Chiayi, Taiwan
[d] Chang-Gung University College of Medicine, Taoyuan, Taiwan
[e] Department of Radiology and BRIC, University of North Carolina at Chapel Hill, Chapel Hill, NC, USA

ARTICLE INFO

Keywords:
Trigeminal neuralgia
Radiofrequency rhizotomy
Functional MRI
Modular organization
Pain chronification

ABSTRACT

Background: The modular organization of brain networks in trigeminal neuralgia patients has remained largely unknown. We aimed to analyze the brain modules and intermodule connectivity in patients with trigeminal neuralgia before and after percutaneous radiofrequency rhizotomy treatment to identify specific modules that may be associated with the development and brain plasticity of trigeminal neuralgia and to test the ability of modularity analysis to be a predictive imaging biomarker for the treatment effect in patients with trigeminal neuralgia.

Methods: A total of 25 patients with right trigeminal neuralgia and 20 matched healthy subjects were included. Blood-oxygen-level dependent resting state fMRI was used to analyze the brain modular organization.

Results: Whole brain modularity analysis identified seven modules. The metric of intermodule connectivity, participation coefficient, of the sensorimotor network and default mode network modules were significantly lower in patients and increased after surgery. The participation coefficient of the subcortical modules was associated with the pain duration. Higher communication between the default mode network module and other modules before surgery was associated with a better treatment response. Furthermore, the subcortical module was a significant contributor to the participation coefficient relationship of the default mode network module with the treatment response, and the bilateral midcingulate cortex and thalamus were major connectors in the subcortical module.

Conclusions: These findings have important implications regarding the global brain modular responses to chronic neuropathic pain and it may be feasible to use the modularity analysis as part of a risk stratification to predict the treatment response.

1. Introduction

Only few neuroimaging studies have focused on the structural and functional changes of the brain in classical TN and the reported results were heterogeneous. Reduced gray matter (GM) volume were found in the sensorimotor cortex (SMC), orbitofrontal cortices, thalamus, insula, anterior cingulate cortex (ACC), cerebellum, dorsolateral prefrontal cortex (PFC), hippocampus, dorsal anterior cingulate cortex, precuneus, and several areas of the temporal lobe (Obermann et al., 2013;Wang et al., 2018;Tsai et al., 2018), and increased GM volume was found in the sensory thalamus, amygdala, periaqueductal GM, putamen, caudate and nucleus accumbens (Desouza et al., 2013). Recent studies using resting state fMRI (rs-fMRI) by Wang et al. showed the altered amplitude of low-frequency fluctuation in the temporal occipital, frontal, cingulate gyrus (Wang et al., 2017). Another study by Yuan et al. reported a significant change in regional homogeneity and fractional amplitude of low-frequency fluctuation in the cerebellum, cingulate cortex, temporal lobe, putamen, occipital lone, limbic lobe, precuneus, insula and frontal gyrus in TN patients (Yuan et al., 2018). Previous studies have demonstrated that the human brain can not only be parsed into networks but also that interactions within and between networks are altered in chronic back pain patients (Balenzuela et al., 2010) and in patients with somatoform pain disorder (Otti et al., 2013). Besides, the interaction of regions or nodes in networks could be organized into and functions as a modular organization by using graph theory-based analyses, which supports segregation and integration of

* Corresponding author.
E-mail address: limingh@ad.unc.edu (L.-M. Hsu).

https://doi.org/10.1016/j.nicl.2019.102027
Received 13 June 2019; Received in revised form 22 August 2019; Accepted 2 October 2019
Available online 21 October 2019

communication between nodes (Sporns, 2013;Bullmore and Sporns, 2009). However, the connection between different brain regions or networks in patients of TN has seldom been discussed, motivating further work to evaluate possible global changes in the brain modular organization of these patients.

Developments in the analysis of complex networks, based largely on graph theory, have suggested that the brain is organized and functions as a complex network of anatomically connected and functionally interacting regions (Bullmore and Sporns, 2009). Recent graph theory-based analyses suggest a modular architecture of the brain that supports segregation and integration of communication among highly connected brain regions (or nodes) (Sporns, 2013). In this context, modularity refers to the level to which a network is organized into modules or communities, such that a module in a network is defined as a set of nodes that are densely connected within a module and sparsely connected to nodes outside of the module (Newman, 2006).

The current study uses rs-fMRI to achieve two specific aims. The first aim is to analyze the brain modules and intermodule connectivity in patients with TN before and after percutaneous radiofrequency rhizotomy (RFA) treatment to relieve their facial pain. This can help to identify specific modules and intermodule connectivity that may be associated with the development and brain plasticity of this specific type of chronic neuropathic orofacial pain and to see how it responses to therapy. The second aim is to analyze the association between the pretreatment intermodule connectivity and the treatment outcome. This will test the ability of modularity analysis to be a predictive imaging biomarker for the treatment effect in patients with TN.

2. Materials and methods

2.1. Subjects

Twenty-five patients with right TN were prospectively enrolled. All patients were diagnosed with classical TN according to the criteria of the International Headache Society for TN, 3rd edition (Headache Classification Committee of the International Headache Society (IHS), 2013). All of the enrolled patients were right-handed with age ranged from 40 to 70 years-old. Patients with past histories of any neurological disease other than TN, such as chronic headache, stroke, brain tumor, seizure disorders, or any pathological findings in conventional MRI were excluded. The age, gender and the duration patient suffered with TN were recorded and the severity of pain was rated based on the visual analogue scale (VAS) pain score. Patients on analgesic medication were asked to discontinue their medication one day before their scheduled scanning session. In addition, 20 healthy subjects (HS) without histories of neurological disease or any pathological findings in conventional MRI were enrolled. Part of the MRI data of HS and TN patients before treatment had been analyzed and presented in our previous study for different aims and with different methods(Tsai et al., 2018). The study was approved by the Institutional Review Board of Chang Gung Medical Foundation and all patients gave their written informed consent prior to their participation in the study.

2.2. Radiofrequency rhizotomy

Percutaneous CT-guided RFA was performed by an experienced neurosurgeon. The rhizotomy needle was inserted into the location confirmed by reproduction of paresthesia upon stimulation, covering the distribution of a specific division of the trigeminal nerve. A lesion was made at the Gasserian ganglion by radiofrequency thermocoagulation (Radionics, Inc. Burlington, MA, USA) at 60 °C for 60 s. The same neurosurgeon rated the severity of pain and treatment effect of patients with VAS pain scores at the time point before the two MRI scans that was within one week before rhizotomy (Pre- VAS) and 2 weeks after rhizotomy (Follow-up VAS)

2.3. MRI acquisition

All patients and healthy controls underwent MRI in a 3-T Siemens Verio MRI system (Siemens Medical System, Erlangen, Germany) using a 32-channel head coil. The MRI protocol was performed within one week before the surgery treatment (1st) and at the 2nd week after surgery. 3D MP-RAGE anatomical images were obtained using a gradient echo sequence (TR = 1900 ms; TE = 2.98 ms; FOV = 230 mm; matrix = 220 × 256; slice number = 160; spatial resolution = 0.9 × 0.9 × 0.9 mm). Functional images were obtained using a gradient EPI sequence that is sensitive to blood-oxygen-level-dependent contrast (TR = 2500 ms, TE = 27 ms, FOV = 220 mm, matrix = 64 × 64 × 36, slice thickness = 4 mm. Each scan consisted of 240 image volumes). All subjects were instructed to stay awake and relaxed, with their eyes closed during the scan.

2.4. Data preprocessing

fMRI image preprocessing: The rs-fMRI data preprocessing was conducted in AFNI (Cox, 1996) including slice timing and head motion correction after discarding the first 10 functional volumes. The spike was removed from the time series using 3dDespike in AFNI. Data were then spatially normalized to a template in SPM and resampled resolution of $2 \times 2 \times 2\,mm^3$ and smoothed with a 6 mm full-width half-maximum (FWHM) Gaussian kernel to increase the spatial signal-to-noise ratio. The time courses of the six head motion correction parameters, white matter (WM), and cerebrospinal fluid (CSF) also served as uninteresting covariates. Here, the WM and CSF masks were generated by segmenting the T1 high-resolution structural images in SPM segmentation and thresholded by 0.95. The data were band-pass filtered (0.01–0.1 Hz) using 3dBandpass in AFNI. Finally, we scrubbed the data to reduce motion-related artifacts by using a framewise displacement (FD) threshold of 0.5, and deleting one time point before and two time points after (Power et al., 2015, 2014).

Regions-of-interests: To conduct graph theory-based analyses, we constructed a whole-brain network using regions-of-interest (ROIs) as nodes and functional connectivity (FC) between these ROIs as edges. We used the Shen Brain Atlas, which consists of 268 ROIs of 2-mm dimensions and provides whole-brain coverage of the cerebral cortex, cerebellum, and brainstem (Shen et al., 2013). In this study, 49 ROIs in the cerebellum and 14 ROIs uncovered in our scan were excluded.

Modularity analysis: We assessed the community structure using modularity analysis (Rubinov and Sporns, 2010) on the group-averaged FC matrix from the 205 ROIs. For each subject, we extracted the time course from each ROI (network nodes) and computed the Pearson correlation between every pair of nodes to form the 205 × 205 resting-state FC matrix. Correlation coefficients were converted into Fisher's Z-values before applying algebraic and statistical operations. Next, resting-state FC matrices were averaged across all subjects to produce a mean resting-state FC matrix. To decompose the lowest hierarchy components while maintaining that there were no isolated nodes in the whole-brain network, the matrix was thresholded at $r = 0.35$ ($p < 0.001$, Bonferroni corrected) to keep the strongest connections (Hsu et al., 2016).

Modules refer to groups of nodes that are highly interconnected with each other but less connected with other network nodes. The modularity index Q, quantifies the efficacy of partitioning a network into modules by evaluating the difference between the actual number of intramodule connections and the expected number for the same modules in a randomized network (Newman, 2004). The objective of a modular detection procedure is to find a specific partition that maximizes Q. Newman's spectral algorithm was used for modular detection (Newman, 2006). To examine whether the real modular network was significantly different than random graphs, we randomized the original network with preserved strength distribution 1000 times and calculated the mean (μ) and standard deviation (σ) of those modularity values

(Maslov and Sneppen, 2002). We compared the modularity Q of the real network to those values, which measures how many standard deviations the real modularity is above the mean for the random graph:

$$z = \frac{Q - \mu}{\sigma}$$

In addition, the modules smaller than five ROIs was excluded.

Intermodule connectivity: Modular assignment provides the basis for assessing the patterns of intermodule connectivity. A standard network metric, the participation coefficient (PC), was used to assess intermodule interactions (Guimerà and Amaral, 2005) and was calculated as:

$$PC_i = 1 - \sum_{s=1}^{N_M} \left(\frac{k_{is}}{k_i}\right)^2$$

where N_M is the number of modules, k_{is} is the number of edges linking the node i to other nodes in module s, and k_i is the total degree of the node i. For each module, the averaged PC of nodes within the module was estimated.

2.5. Statistics

One-way analysis of variance (ANOVA) was used to compare the VAS scores among the pre-, post-, and follow-up treatment. For all analyses and *post hoc* comparisons, a $p_{corrected} < 0.05$ was considered significant, and all comparisons were Bonferroni corrected.

Predicting treatment effect by imaging measures: Since we intended to assess whether network measures obtained before treatment predict treatment effects at 2 weeks after rhizotomy (Follow-up VAS), the correlation between the baseline PC and treatment effect score (the changes between Follow-up VAS and Pre-VAS was divided by Pre-VAS) was calculated.

FC between modules: As a *post hoc* analysis, we computed the between-module connectivity for each subject by averaging functional correlations across all pairs of anatomical ROIs between the identified sensorimotor and default mode network (see Results) and all other modules identified by our predictive measure. The FC between modules was correlated with the change in treatment effect.

2.6. Data availability statement

The clinical information and raw data of MRI will be shared by request from any qualified investigator after the permission of the Institutional Review Board of our institution.

3. Results

3.1. Clinical characteristics

Clinical characteristics are listed in Table 1. There was no significant difference between the HS and TN patients in terms of age, sex, handedness, or education years. However, there was a significant difference in the VAS score of TN patients between the Pre- and follow-up treatment ($p < 0.001$, paired samples t-test).

3.2. Whole-brain modularity analysis

Modularity analysis of the group-averaged FC matrix across HS and TN group revealed seven brain modules as: frontal-parietal network (FPCN), sensorimotor network (SMN), salience network (SN), default mode network (DMN), ventral-DMN (vDMN), visual, and subcortical modules (Fig. 1a).

Among the seven brain modules, the SMN and DMN showed significantly decreased participation coefficient (PC) between the HS and TN patients before surgery (Fig. 1b). There was no significant PC difference between the HS and TN patients after surgery. Overall, the PC value of all the seven brain modules showed an increasing trend after surgery in the patient group. In addition, before treatment, only the subcortical module showed significant association between the PC and pain duration (Fig. 1c).

Table 1
Demographics and patient characteristics.

Number of patients	Patient (n = 25)	Healthy Subject (n = 20)	p-value
Age, years (mean ± SD)	58.7 ± 6.0	55.7 ± 7.8	0.143
Sex (female/male)	15/10	13/7	0.731
Pain location V1/V2/V3 (%)	16/76/76	n.a.	
Pain duration, months (mean ± SD)	85.7 ± 86.1	n.a.	
Pain intensity (VAS)			<0.001*
Pre-	9.3 ± 0.7	n.a.	
Follow-up	3.0 ± 2.9	n.a.	

VAS, visual analog scale.
Pain duration, time for the patient suffered from trigeminal neuralgia.
* Difference between the Pre- and Follow-up VAS scores by paired sample t-test.

3.3. Association between modularity analysis and the treatment outcome

Given that the SMN and DMN were the only two modules identified to show significant PC changes in patient groups before surgery, we used only these two modules to test whether they could predict the treatment effect (the difference between the VAS score before surgery and at 2 weeks after surgery was divided by the score before surgery). Of the two identified modules, only the PC of the DMN at baseline correlated significantly ($r = 0.42$, $p_{corrected} < 0.05$) with the treatment effect score (Fig. 2), suggesting that patients with better communication between the DMN and all other modules before surgery may benefit more from the treatment.

3.4. Post hoc analysis of the functional connectivity of the DMN module with other identified brain modules

To determine which of the remaining brain modules connected to the DMN module were most associated with the treatment effect, stepwise linear regression was performed as a *post hoc* analysis between functional connectivity (FC) of the DMN module with other identified brain modules and the treatment effect score. We found that the FC between the DMN and subcortical modules (Fig. 3) before surgery was a significant predictor of the changes in the VAS score before and after treatment ($r = -0.72$, $p_{corrected} < 0.001$), accounting for 52% of the variance in this model.

The normalized PC value for each node in the subcortical and DMN modules is listed in Fig. 4. The right midcingulate cortex (R-mCing), left middle thalamus (L-mThal), left midcingulate cortex (L-mCing), and right middle thalamus (R-mThal) showed higher PC values than the other nodes in the subcortical module, which indicated that the four nodes were major connectors in the subcortical module. In the DMN module, seven connectors were identified, which included the inferior parietal lobule (R-iPar and L-iPar), inferior frontal gyrus (R-iFront and L-iFront), middle frontal gyrus (L-mFront), middle temporal gyrus (R-mTemp), and inferior temporal gyrus (L-miTemp).

4. Discussion

Graph-based network analyses have been used to investigate organizational mechanism underlying the relevant networks (Wang et al., 2010). Modularity analysis can reflect the degree to which a network is organized into a modular or community structure (Newman, 2006).

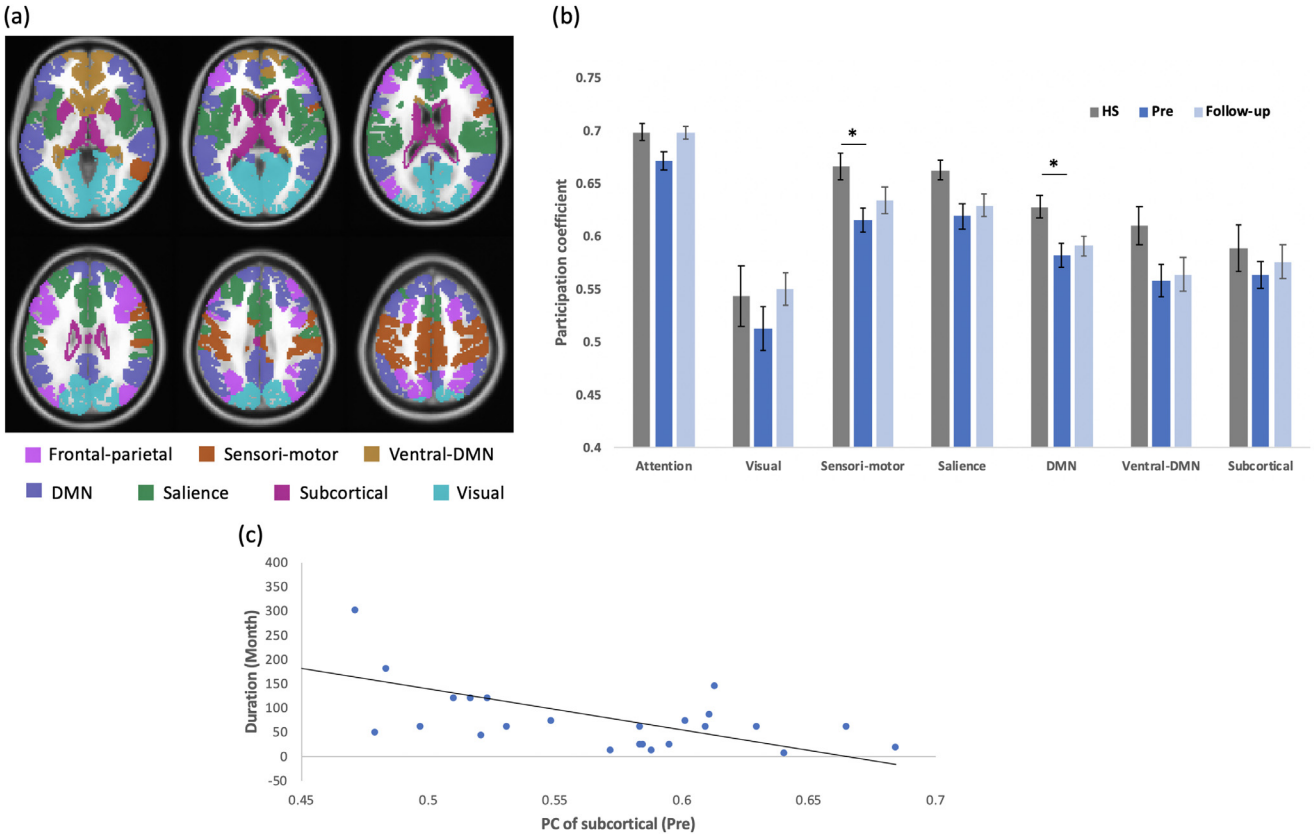

Fig. 1. (a) Modular structure of functional networks with brain regions color-coded according to their modular affiliation with underlay of anatomical image. (b) Mean participation coefficient (PC) of each module across HS and TN patients. Among the 7 modules, only the sensorimotor and DMN showed significant decrease in PC in Pre-RFA group compared with HC and no significant difference between HC and the Follow-up group. (*, $p_{corrected} < 0.05$). (c) PC of the subcortical module showed a significant association with pain duration ($r = -0.63$, $p_{corrected} < 0.01$). The error bar indicated the standard error.

Measurement of the modules can not only describe the presence of densely interconnected groups of regions but also find the exact size and composition of these individual groups. This is known as the network's modular structure, which can subdivide the network into groups of nodes (Rubinov and Sporns, 2010). Based on the identified modular structure, hubs can be further subdivided in terms of their roles in maintaining intra or intermodule connectivity. In contrast to other widely used rs-fMRI analytic methods, such as seed-based functional connectivity, independent component analysis, amplitude of low-frequency and regional homogeneity, the graph-based network analyses allow us not only to see the individual connectivity among all the elements (regions or networks) of the brain, but to also quantitatively characterize the global organization.

Studies of a variety of pain processes have shown the decrease or reorganization of the intrinsic DMN activity as a characteristic change of acute and chronic pain (Hemington et al., 2018;Alshelh et al., 2018). The role of cross-network functional connectivity of the DMN in pain has also been reported. In a study of somatoform pain disorder, Otti et al. found alteration of the FC between the DMN, SMC and cingular-insular network (Otti et al., 2013). Loggia et al. reported that severe symptoms of chronic low back pain were associated with the strength of the FC between the DMN and the insula (Loggia et al., 2013). Another study by Liu et al. showed altered connectivity between the DMN and PFC, ACC and thalamus in patients with primary dysmenorrhea (Liu et al., 2017). The SMN has been shown to code the location and intensity of pain stimuli and is the key driver for motor responses or

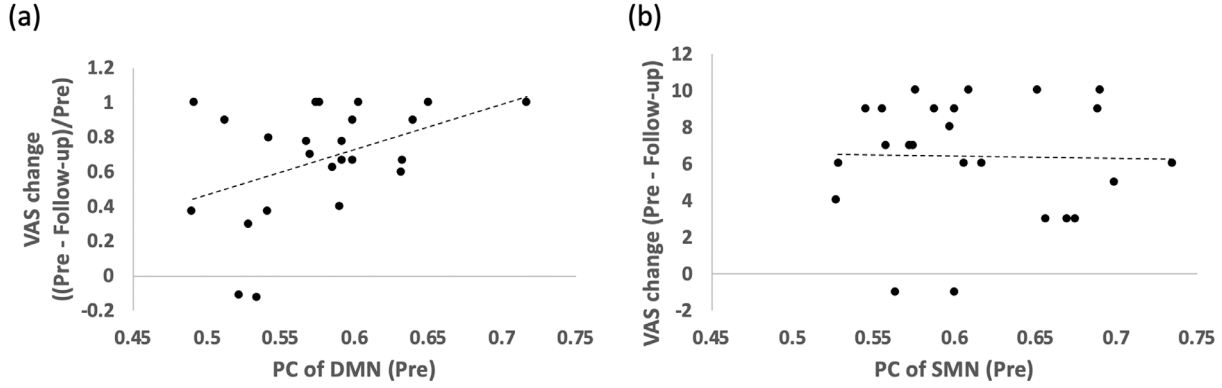

Fig. 2. Among DMN and SMN modules, only the PC of the DMN module (a) showed significant correlation with changes of VAS score from Pre to Follow-up ($r = 0.42$, $p_{corrected} < 0.05$). There was no significant relationship between PC of the SMN module (b) and changes of VAS score from Pre to follow-up ($r = -0.01$).

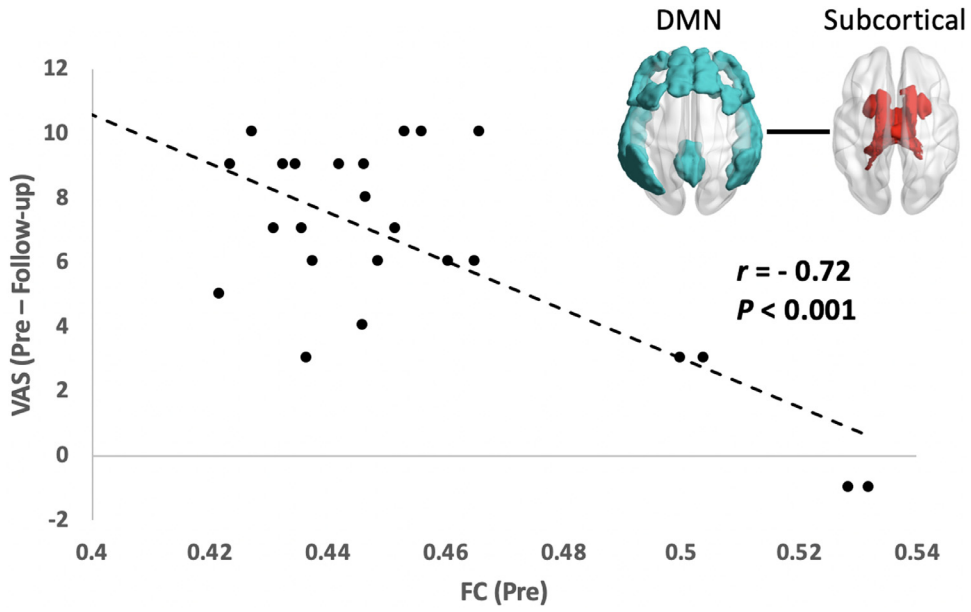

Fig. 3. FC of the DMN module with the subcortical module ($r = -0.72$, $p_{corrected} < 0.001$) was negatively correlated with the change in VAS score (pre – follow-up).

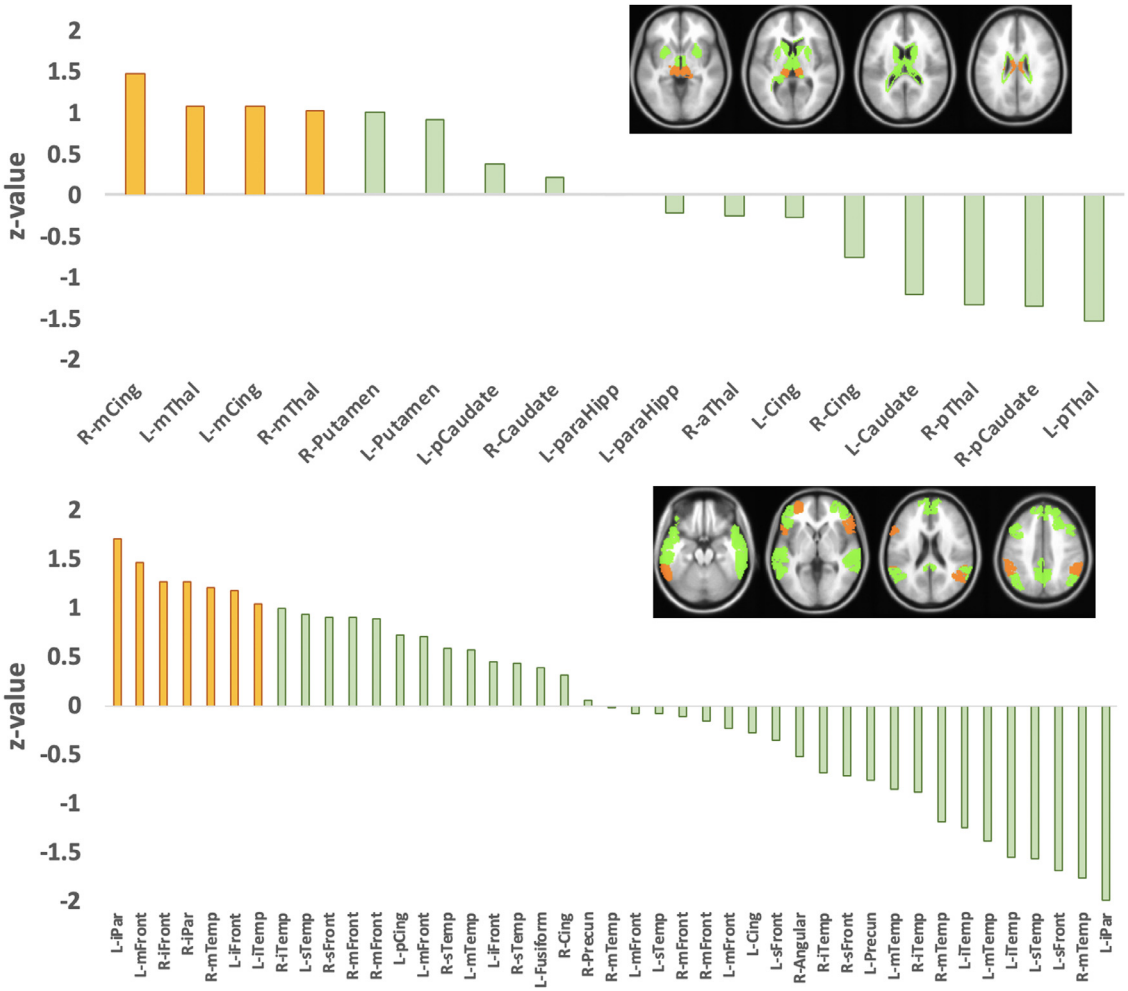

Fig. 4. Normalized PC value for each node in the subcortical module (upper row) and DMN module (lower row). The threshold was set as z-value = 1 (orange color). In the subcortical module, the high PC value of middle cingulate (R-mCing and L-mCing) and middle thalamus (L-mThal and R-mThal) represented the major connector. In the DMN module, the high PC value of the inferior parietal lobule (R-iPar and L-iPar), inferior frontal gyrus (R-iFront and L-iFront), middle frontal gyrus (L-mFront), middle temporal gyrus (R-mTemp), and the inferior temporal gyrus (L-miTemp) represented the major connector. (For interpretation of the references to color in this figure legend, the reader is referred to the web version of this article.)

movement dysfunction in pain (Chang et al., 2015;Bushnell et al., 2013). A study of patients with somatoform pain disorder showed increased coactivations in the bilateral supplementary motor areas within the SMN and a decreased FC between the SMN and both audio and visual networks (Zhao et al., 2017). Another study by Hemington et al. showed a high FC between the DMN and SMN in chronic pain patients with high clinical pain scores (Hemington et al., 2018). Our previous study showed that the FC between dorsal lateral PFC and primary motor cortex was higher in patients of TN and this connectivity is negatively correlated with the duration of pain (Tsai et al., 2018). In the current study, the PC of the DMN and SMN were significantly lower in TN patients compared to the normal subjects. This result confirms the roles of these networks in patients with this specific type of chronic neuropathic pain. These networks are not only responsible for processing the pain signal (as TN is a brief paroxysmal pain) but also involved in functional modulation or plasticity of the brain in response to the chronic pain signal. The low PC indicates low intermodule interactions between the SMN, DMN and other brain modules, which may decrease the delivery of the pain signal and may be an intrinsic response to reduce the sensation of pain. One of the mechanisms of TN is long-term and pulsatile compression of the trigeminal nerve by vessels that leads to focal demyelination and transform juxtaposition of axons, which also causes ectopic generation of spontaneous nerve impulses into adjacent fibers that initiates pain signals (Smith and McDonald, 1980;Love and Coakham, 2001). Another explanation of the low PC of the SMN and DMN modules may be due to the inhibitive signals from the abnormal spontaneous nerve impulses. Interestingly, the PC of the SMN and DMN, as well as other measured modules, increased after surgery, while relief of pain was achieved in most patients. The reason for that all the intermodular connection showed recovery trend after surgery but did not reach a statistic significance may be that all patients suffered from repeated chronic pain for several months to years and the responses or plasticity of some of the modules may be a chronic process that can't be completely recovered after a single treatment, not to say some patients had only partial recovery and the time of the follow-up scan was just at 2 weeks after rhizotomy.

We observed that a higher interaction between the DMN and other modules before surgery was associated with a better treatment response. In recurrent and severe TN patients, affected trigeminal nerves have been observed to be distorted and with an atrophic pattern, which was caused by inflammation and edema that progressed to demyelination, abnormal remyelination and hypermyelination (Love and Coakham, 2001). As our surmises above, the abnormal low PC between DMN and other brain models may be due to the inhibitive signals from the abnormal spontaneous nerve impulses or an intrinsic functional modulation to reduce pain, a lower PC of the DMN module before surgery may indicate more critical neural damage with a stronger impulse of the pain signal that makes the nerve and symptoms more refractory to the RFA treatment.

Among the remaining brain modules, the FC between the subcortical module and the DMN module was most associated with the prediction, accounting for 52% of the variance in this model. The subcortical structures are known to be involved in a variety of aspect of pain perception and modulation (Bushnell et al., 2013;Vogt, 2005;Bingel et al., 2002). We further found that the bilateral midcingulate cortex (MCC) and thalamus were the major connectors in the subcortical nodules. As we mentioned above, the thalamus plays a key role in the processing of nociceptive stimuli by projection of nociceptive input from the thalamus to the SMC, ACC, insula and other cortical regions (Bushnell et al., 2013). Studies have also shown that chronic pain disrupts thalamo-cortical connections (Cauda et al., 2014;Jensen et al., 2012). The cingulate cortex is consistently activated in nociception in human and animal studies and has been shown to be responsible for the transition from acute to chronic pain. It has been regarded as a central hub in the pain matrix and is highly connected to most other brain areas involved in the processing of pain (Nevian, 2017). The cingulate cortex has 4 sub-regions and each or them is response for different aspects of pain processing and modulation. Among them, MCC is involved with the sensory processing and response selection (Vogt, 2005;Nevian, 2017). A recent animal study by Tan et al. showed that the MCC gates sensory hypersensitivity by acting in a wide cortical and subcortical networks (Tan et al., 2017). They also identified a connection from the MCC to the posterior insula that can induce and maintain nociceptive hypersensitivity in the absence of conditioned peripheral noxious stimulation. Thus, the MCC may act as a hub for activating the associated networks to facilitate the transition from acute to long-lasting pain.

Interestingly, the results of our current study show that the PC of the subcortical modules was associated with the duration that the patient suffered from TN. The PC of subcortical modules for patients with longer pain duration was higher than those with shorter pain duration. This might concur with the results of a previous study that showed that the subcortical structures play a role in pain chronification. A recent magnetic resonance spectroscopy study by Niddam et al. showed reduced N-acetyl-aspartate metabolism and altered interregional N-acetyl-aspartate correlations in thalamus, cingulate and occipital cortex among migraine patients, which supports the role of thalamocortical dysfunction in migraine chronification (Niddam et al., 2018). We also found that a lower FC between the DMN and subcortical modules was associated with a better treatment response and the thalamus and midcingulate cortex were the major connectors within the subcortical module. As the thalamus and MCC both play important roles in encoding the emotional and motivational aspects of pain, as well as chronification of pain by projecting the nociceptive input to other brain regions or networks, the lower FC between the DMN and subcortical modules may indicate a minor encoding or chronification of the chronic nociceptive input signal, which can be eliminated more easily by RFA.

We recognize some limitations in this study. Although we only included patients with right side TN to exclude the effect of pain laterization, the pain characteristics, such as pain intensity and pain distribution, were mixed in the patient group. Next, we chose VAS pain scores as the rating scale for representing the treatment effect although the pain behavior could also be measured with other instruments, including the Pain Rating Scale (PRS) and Pain Behavior Checklist (PBC) (Dirks et al., 1993). These approaches could benefit further discussion from the diverse phenomenology of trigeminal neuralgia. Furthermore, the experimental design did not take the placebo effect into consideration and findings from MRI analysis and clinical pain score might not only from the effect of intervention but also the patients' subjective feelings.

In conclusion, our results from a graph theory modularity analysis of rs-fMRI suggest the PC of the SMN and DMN were significantly lower in TN patients and increased after surgery, which may be due to a decrease in the transduction of the pain signal or the inhibitive signal from the abnormal spontaneous sensory impulse of the trigeminal nerve. The higher communication between the DMN module and other modules before surgery was associated with better treatment response to RFA. The PC of the subcortical modules was associated with pain duration. A lower connection between the DMN and subcortical modules was associated with a better treatment response and the thalamus and midcingulate cortex were the major connectors within the subcortical module. These results have important implications regarding the global brain modular responses to chronic neuropathic pain and it may be feasible to use the modularity analysis as part of a risk stratification to predict the response of patients to RFA therapy.

Declaration of Competing Interest

None.

Fundingt

This study was supported by Chang Gung Medical Foundation CMRPG6C0282 and CMRPG6F0531.

References

Alshelh, Z., Marciszewski, K.K., Akhter, R., Di Pietro, F., Mills, E.P., Vickers, E.R., Peck, C.C., Murray, G.M., Henderson, L.A., 2018. Disruption of default mode network dynamics in acute and chronic pain states. NeuroImage Clin. 17, 222–231. https://doi.org/10.1016/j.nicl.2017.10.019.

Balenzuela, P., Chernomoretz, A., Fraiman, D., Cifre, I., Sitges, C., Montoya, P., Chialvo, D.R., 2010. Modular organization of brain resting state networks in chronic back pain patients. Front. Neuroinform 4. https://doi.org/10.3389/fninf.2010.00116.

Bingel, U., Quante, M., Knab, R., Bromm, B., Weiller, C., Buchel, C., 2002. Subcortical structures involved in pain processing: evidence from single-trial fMRI. Pain 99, 313–321.

Bullmore, E., Sporns, O., 2009. Complex networks: graph theoretical analysis of structural and functional systems. Nat. Rev. Neurosci. 10, 186–198. https://doi.org/10.1038/nrn2575.

Bushnell, M.C., Čeko, M., Low, L.A., 2013. Cognitive and emotional control of pain and its disruption in chronic pain. Nat. Rev. Neurosci. 14, 502–511. https://doi.org/10.1038/nrn3516.

Cauda, F., Palermo, S., Costa, T., Torta, R., Duca, S., Vercelli, U., Geminiani, G., Torta, D.M.E., 2014. Gray matter alterations in chronic pain: a network-oriented meta-analytic approach. NeuroImage Clin 4, 676–686. https://doi.org/10.1016/j.nicl.2014.04.007.

Chang, W., O'Connell, N.E., Burns, E., Chipchase, L.S., Liston, M.B., Schabrun, S.M., 2015. Organisation and function of the primary motor cortex in chronic pain: protocol for a systematic review and meta-analysis. BMJ Open 5, e008540. https://doi.org/10.1136/bmjopen-2015-008540.

Desouza, D.D., Moayedi, M., Chen, D.Q., Davis, K.D., Hodaie, M., 2013. Sensorimotor and pain modulation brain abnormalities in trigeminal neuralgia: a paroxysmal, sensory-triggered neuropathic pain. PLoS One 8, e66340. https://doi.org/10.1371/journal.pone.0066340.

Dirks, J.F., Wunder, J., Kinsman, R., McElhinny, J., Jones, N.F., 1993. A pain rating scale and a pain behavior checklist for clinical use: development, norms, and the consistency score. Psychother. Psychosom. 59, 41–49. https://doi.org/10.1159/000288643.

Guimerà, R., Amaral, L.A.N., 2005. Functional cartography of complex metabolic networks. Nature 433, 895–900. https://doi.org/10.1038/nature03288.

Headache Classification Committee of the International Headache Society (IHS), 2013. The international classification of headache disorders, 3rd edition (beta version). Cephalalgia 33, 629–808. https://doi.org/10.1177/0333102413485658.

Hemington, K.S., Rogachov, A., Cheng, J.C., Bosma, R.L., Kim, J.A., Osborne, N.R., Inman, R.D., Davis, K.D., 2018. Patients with chronic pain exhibit a complex relationship triad between pain, resilience, and within- and cross-network functional connectivity of the default mode network. Pain 159, 1621–1630. https://doi.org/10.1097/j.pain.0000000000001252.

Hsu, L.-.M., Liang, X., Gu, H., Brynildsen, J.K., Stark, J.A., Ash, J.A., Lin, C.-.P., Lu, H., Rapp, P.R., Stein, E.A., Yang, Y., 2016. Constituents and functional implications of the rat default mode network. Proc. Natl. Acad. Sci. USA. 113, E4541–E4547. https://doi.org/10.1073/pnas.1601485113.

Jensen, K.B., Loitoile, R., Kosek, E., Petzke, F., Carville, S., Fransson, P., Marcus, H., Williams, S.C.R., Choy, E., Mainguy, Y., Vitton, O., Gracely, R.H., Gollub, R., Ingvar, M., Kong, J., 2012. Patients with fibromyalgia display less functional connectivity in the brain's pain inhibitory network. Mol. Pain 8, 32. https://doi.org/10.1186/1744-8069-8-32.

Liu, P., Liu, Y., Wang, G., Yang, X., Jin, L., Sun, J., Qin, W., 2017. Aberrant default mode network in patients with primary dysmenorrhea: a fMRI study. Brain Imaging Behav. 11, 1479–1485. https://doi.org/10.1007/s11682-016-9627-1.

Loggia, M.L., Kim, J., Gollub, R.L., Vangel, M.G., Kirsch, I., Kong, J., Wasan, A.D., Napadow, V., 2013. Default mode network connectivity encodes clinical pain: an arterial spin labeling study. Pain 154, 24–33. https://doi.org/10.1016/j.pain.2012.07.029.

Love, S., Coakham, H.B., 2001. Trigeminal neuralgia: pathology and pathogenesis. Brain 124, 2347–2360. https://doi.org/10.1093/brain/124.12.2347.

Maslov, S., Sneppen, K., 2002. Specificity and stability in topology of protein networks. Science 296, 910–913. https://doi.org/10.1126/science.1065103.

Nevian, T., 2017. The cingulate cortex: divided in pain. Nat. Neurosci. 20, 1515.

Newman, M.E.J., 2006. Modularity and community structure in networks. Proc. Natl. Acad. Sci. USA 103, 8577–8582. https://doi.org/10.1073/pnas.0601602103.

Newman, M.E.J., 2004. Analysis of weighted networks. Phys. Rev. E. Stat. Nonlinear Soft Matter Phys. 70, 056131. https://doi.org/10.1103/PhysRevE.70.056131.

Niddam, D.M., Lai, K.-.L., Tsai, S.-.Y., Lin, Y.-.R., Chen, W.-.T., Fuh, J.-.L., Wang, S.-.J., 2018. Neurochemical changes in the medial wall of the brain in chronic migraine. Brain 141, 377–390. https://doi.org/10.1093/brain/awx331.

Obermann, M., Rodriguez-Raecke, R., Naegel, S., Holle, D., Mueller, D., Yoon, M.-.S., Theysohn, N., Blex, S., Diener, H.-.C., Katsarava, Z., 2013. Gray matter volume reduction reflects chronic pain in trigeminal neuralgia. Neuroimage 74, 352–358. https://doi.org/10.1016/j.neuroimage.2013.02.029.

Otti, A., Guendel, H., Henningsen, P., Zimmer, C., Wohlschlaeger, A.M., Noll-Hussong, M., 2013. Functional network connectivity of pain-related resting state networks in somatoform pain disorder: an exploratory fMRI study. J. Psychiatry Neurosci. 38, 57–65. https://doi.org/10.1503/jpn.110187.

Power, J.D., Mitra, A., Laumann, T.O., Snyder, A.Z., Schlaggar, B.L., Petersen, S.E., 2014. Methods to detect, characterize, and remove motion artifact in resting state fMRI. Neuroimage 84, 320–341. https://doi.org/10.1016/j.neuroimage.2013.08.048.

Power, J.D., Schlaggar, B.L., Petersen, S.E., 2015. Recent progress and outstanding issues in motion correction in resting state fMRI. Neuroimage. https://doi.org/10.1016/j.neuroimage.2014.10.044.

Rubinov, M., Sporns, O., 2010. Complex network measures of brain connectivity: uses and interpretations. Neuroimage 52, 1059–1069. https://doi.org/10.1016/j.neuroimage.2009.10.003.

Shen, X., Tokoglu, F., Papademetris, X., Constable, R.T., 2013. Groupwise whole-brain parcellation from resting-state fMRI data for network node identification. Neuroimage 82, 403–415. https://doi.org/10.1016/j.neuroimage.2013.05.081.

Smith, K.J., McDonald, W.I., 1980. Spontaneous and mechanically evoked activity due to central demyelinating lesion. Nature 286, 154–155.

Sporns, O., 2013. Network attributes for segregation and integration in the human brain. Curr. Opin. Neurobiol. https://doi.org/10.1016/j.conb.2012.11.015.

Tan, L.L., Pelzer, P., Heinl, C., Tang, W., Gangadharan, V., Flor, H., Sprengel, R., Kuner, T., Kuner, R., 2017. A pathway from midcingulate cortex to posterior insula gates nociceptive hypersensitivity. Nat. Neurosci. 20, 1591–1601. https://doi.org/10.1038/nn.4645.

Tsai, Y.H., Yuan, R., Patel, D., Chandrasekaran, S., Weng, H.H., Yang, J.T., Lin, C.P., Biswal, B.B., 2018. Altered structure and functional connection in patients with classical trigeminal neuralgia. Hum. Brain Mapp. 39, 609–621. https://doi.org/10.1002/hbm.23696.

Vogt, B.A., 2005. Pain and emotion interactions in subregions of the cingulate gyrus. Nat. Rev. Neurosci. 6, 533–544. https://doi.org/10.1038/nrn1704.

Wang, J., Zuo, X., He, Y., 2010. Graph-based network analysis of resting-state functional MRI. Front. Syst. Neurosci. 4, 16. https://doi.org/10.3389/fnsys.2010.00016.

Wang, Y., Xu, C., Zhai, L., Lu, X., Wu, X., Yi, Y., Liu, Z., Guan, Q., Zhang, X., 2017. Spatial-Temporal signature of resting-state bold signals in classic trigeminal neuralgia. J. Pain Res. 10, 2741–2750. https://doi.org/10.2147/JPR.S143734.

Wang, Y., Yang, Q., Cao, D., Seminowicz, D., Remeniuk, B., Gao, L., Zhang, M., 2018. Correlation between nerve atrophy, brain grey matter volume and pain severity in patients with primary trigeminal neuralgia. Cephalalgia. https://doi.org/10.1177/0333102418793643. 333102418793643.

Yuan, J., Cao, S., Huang, Y., Zhang, Yi, Xie, P., Zhang, Yu, Fu, B., Zhang, T., Song, G., Yu, T., Zhang, M., 2018. Altered spontaneous brain activity in patients with idiopathic trigeminal neuralgia: a resting-state functional MRI study. Clin. J. Pain 34, 600–609. https://doi.org/10.1097/AJP.0000000000000578.

Zhao, Z., Huang, T., Tang, C., Ni, K., Pan, X., Yan, C., Fan, X., Xu, D., Luo, Y., 2017. Altered resting-state intra- and inter- network functional connectivity in patients with persistent somatoform pain disorder. PLoS One 12. https://doi.org/10.1371/journal.pone.0176494.